

A review of imaging modalities in pulmonary hypertension

Mona Ascha, Rahul D. Renapurkar¹, Adriano R. Tonelli

Department of
Pulmonary, Allergy
and Critical Care
Medicine, Respiratory
Institute, Cleveland
Clinic, ¹Department of
Diagnostic Radiology,
Cleveland Clinic,
Cleveland, OH, USA

**Address for
correspondence:**

Dr. Adriano R. Tonelli,
Department of Pulmonary,
Allergy and Critical Care
Medicine, Respiratory
Institute, Cleveland Clinic,
9500 Euclid Avenue,
A-90, Cleveland,
OH 44195, USA.
E-mail: tonella@ccf.org

Submission: 25-07-2016
Accepted: 10-11-2016

Abstract:

Pulmonary hypertension (PH) is defined as resting mean pulmonary artery pressure ≥ 25 mmHg measured by right heart catheterization. PH is a progressive, life-threatening disease with a variety of etiologies. Swift and accurate diagnosis of PH and appropriate classification in etiologic group will allow for earlier treatment and improved outcomes. A number of imaging tools are utilized in the evaluation of PH, such as chest X-ray, computed tomography (CT), ventilation/perfusion (V/Q) scan, and cardiac magnetic resonance imaging. Newer imaging tools such as dual-energy CT and single-photon emission computed tomography/computed tomography V/Q scanning have also emerged; however, their place in the diagnostic evaluation of PH remains to be determined. In general, each imaging technique provides incremental information, with varying degrees of sensitivity and specificity, which helps suspect the presence and identify the etiology of PH. The present study aims to provide a comprehensive review of the utility, advantages, and shortcomings of the imaging modalities that may be used to evaluate patients with PH.

Key words:

Imaging, pulmonary hypertension, pulmonary vasculature, review, right ventricle

Pulmonary hypertension (PH) is a progressive, life-threatening, pulmonary vascular condition with a wide array of etiologies and comorbidities.^[1,2] PH is defined as resting mean pulmonary artery pressure (mPAP) ≥ 25 mmHg measured by right heart catheterization (RHC), the gold standard for diagnosis.^[2,3] The exact incidence and prevalence of all types of PH is unknown.^[4] According to registry-based data, pulmonary arterial hypertension (PAH) has an estimated prevalence of 10–52 cases/million.^[3] While prognosis depends on the underlying disease etiology, mortality rates, particularly for patients with PAH, remain high despite therapy.^[5]

Over the years, task forces have been updating the recommendations for the classification, diagnosis, and workup of PH patients. The Fifth World Symposium on Pulmonary Hypertension classifies PH into five groups according to disease manifestation, pathophysiology, hemodynamic changes, and therapeutic approaches: Group 1: PAH, Group 2: PH due to left heart disease, Group 3: PH due to lung disease, Group 4: Chronic thromboembolic PH (CTEPH), and Group 5: A miscellaneous group of PH with unclear or multifactorial mechanisms.^[1] The diagnosis of PH is based on a comprehensive evaluation of clinical symptoms, physical examination, and imaging modalities. Unfortunately, diagnosis of PH, and thus its treatment, is often delayed, as clinical symptoms overlap with more prevalent respiratory and cardiovascular diseases.^[6]

Familiarity with imaging techniques, knowledge of key findings, and awareness of nuances of imaging studies in PH is imperative since they have the potential for accelerating diagnosis and initiation of PH-specific therapies, an approach that is likely to improve the prognosis of this deadly disease.^[7]

Imaging in PH can be used for three main purposes: (1) suspecting the presence of PH, (2) determining the etiology of disease, and (3) evaluating prognosis and response to therapy. The present review aims to provide a comprehensive overview of the utility, advantages, and shortcomings of a multitude of imaging modalities that may be used to evaluate patients with PH.

This is an open access article distributed under the terms of the Creative Commons Attribution-NonCommercial-ShareAlike 3.0 License, which allows others to remix, tweak, and build upon the work non-commercially, as long as the author is credited and the new creations are licensed under the identical terms.

For reprints contact: reprints@medknow.com

How to cite this article: Ascha M, Renapurkar RD, Tonelli AR. A review of imaging modalities in pulmonary hypertension. *Ann Thorac Med* 2017;12:61-73.

Video Available on:
www.thoracicmedicine.org

Access this article online

Quick Response Code:



Website:
www.thoracicmedicine.org

DOI:
10.4103/1817-1737.203742

Initial Diagnosis of Pulmonary Hypertension

Once the diagnosis of PH is suggested, various tests are available for further evaluation [Table 1].

Transthoracic Doppler echocardiography

Transthoracic Doppler echocardiography (TTE) is typically performed as the initial workup in a patient with suspected PH [Figure 1]. TTE is advantageous in that it is widely available, inexpensive, and safe. TTE can estimate the systolic pulmonary arterial pressure (sPAP) from the peak tricuspid regurgitant jet velocity and the right ventricular size and function^[8] with some limitations.^[9] Importantly, TTE is critical in determining the most common cause of PH in the developed world, i.e., PH due to left heart disease.

Chest X-ray

Chest X-ray (CXR) is usually obtained as a baseline investigation in patients undergoing workup of PH. A normal CXR does not exclude PH; however, a CXR is commonly abnormal in established disease.^[10] CXR findings that support the presence of PH include (1) cardiomegaly due to right atrial (RA) and right ventricle (RV) enlargement as evidenced by reduced retrosternal air space. RV enlargement is seen as obliteration of

clear space on lateral CXR, whereas RA enlargement manifests as prominence of right heart border on frontal projection; (2) dilation of central pulmonary arteries; (3) pruning (loss) of peripheral blood vessels [Figure 2].

Morphologic cardiac changes can be seen on CXR in advanced disease. Right-sided heart strain and resulting hypertrophy manifest as cardiomegaly on imaging. Pericardial effusions can occur in patients with advanced PH and are a sign of poor prognosis.^[11,12] Pericardial effusions can also be seen on CXR and are characterized by an enlarged cardiac silhouette that can be described with as a “waterflask” contour; lateral views may outline the divides among the pericardial fluid, epicardial and pericardial fat.^[13] However, it should be noted that rapidly developing pericardial effusions may not be readily apparent on CXR.^[14]

Prominent central pulmonary arteries are indicative of PH. In long-standing PH, atherosclerotic calcifications may also be visualized along the central arteries.^[15] Furthermore,

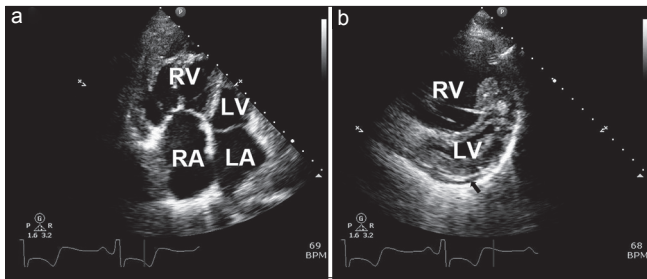


Figure 1: Two-dimensional echocardiogram in a patient with idiopathic pulmonary arterial hypertension. (a) The apical 4-chamber view shows large right heart chambers with hypertrophy of the right ventricle. (b) The short parasternal view with enlarged right ventricle leading to interventricular septal displacement into the left ventricle. The black arrow points toward a small pericardial effusion. LA = left atrium, LV = Left ventricle, RA = right atrium, RV = right ventricle

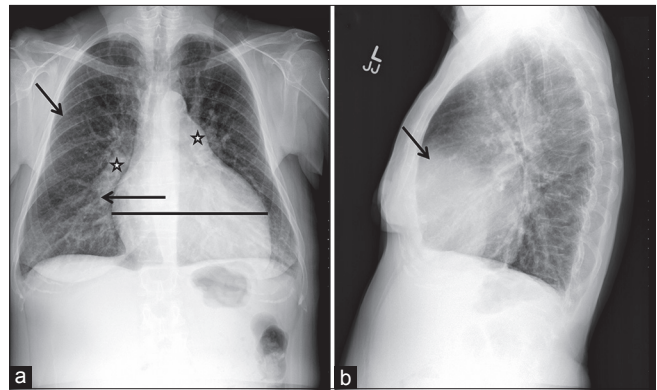


Figure 2: Chest X-ray in a patient with idiopathic pulmonary arterial hypertension. (a) Posteroanterior projection showing dilated pulmonary arteries (stars), cardiomegaly (horizontal line), and rapid tapering (pruning) of right pulmonary artery (arrow). In addition, there is a decrease in the pulmonary vasculature in the periphery of the lung (arrow). (b) Lateral projection depicting a decrease in the retrosternal air space (arrow)

Table 1: Choice of imaging tests in evaluation of pulmonary hypertension

Group	Imaging test of choice	Specific comments
1	Echocardiography (TTE)	IPAH-diagnosis of exclusion Congenital heart disease-bubble echocardiography and shunt study during RHC MRI can play an additional role in defining anatomy; cardiac CT is an alternative Porto-pulmonary hypertension-cirrhosis noted on US/CT
2	Echocardiography (TTE)	Assessment of systolic and diastolic function Valvular heart disease CMRI can play a role in the assessment of myocardial scar and fibrosis
3	CT	Evaluation of lung diseases such as emphysema and ILD
4	V/Q (future-DECT or SPECT-CT V/Q scanning?)	CTA-to define extent of disease and for preoperative planning Echocardiography or TTE/MRI-for evaluation of RV function Pulmonary angiogram-defining anatomy; may be utilized more with success of balloon angioplasty and catheter-based intervention DECT-potential new test of choice
5	CT	Assessment of multifactorial diseases such as sarcoidosis and fibrosing mediastinitis

Once the diagnosis of PH is suggested by echocardiography and confirmed by right heart catheterization; various tests are available for further evaluation. PH = Pulmonary hypertension; TTE = Transthoracic echocardiography; DECT = Dual-energy computed tomography; MRI = Magnetic resonance imaging; RV = Right ventricle; V/Q = Ventilation/perfusion; CT = Computed tomography; ILD = Interstitial lung disease; CMRI = Cardiac magnetic resonance imaging; US = Ultrasound; RHC = Right heart catheterization; IPAH = Idiopathic pulmonary arterial hypertension; SPECT = Single-photon emission computed tomography; CTA = Computed tomography angiography

increased pulmonary artery (PA) – pulmonary vein ratio on CXR – indicates arterial PH, while a decreased one indicates venous PH.^[16] Pruning and rarefaction of peripheral pulmonary vessels is frequently observed in patients with PAH.^[17-19]

In addition to vascular findings related to PH, CXR can be helpful in narrowing the differential diagnosis of its etiology. CXR can be helpful in supporting the diagnosis of left-sided heart disease and for evaluating lung parenchymal diseases such as interstitial lung disease and emphysema. Signs of pulmonary embolism (PE), such as Westermark's sign (a wedge-shaped shadow indicating infarction) or Hampton's hump (a wedge-shaped opacification secondary to hemorrhage), may denote the need for further workup for CTEPH, since approximately 0.6%–3.8% of acute PE events lead to CTEPH.^[20] In one study of 36 patients, characteristic CXR findings of focal areas of avascularity or enlarged right descending PA (diameter >20 mm) together with pleuritic changes, such as pleuritic scarring and pleuritic shadow due to prior pulmonary infarction, were found more commonly in CTEPH than in idiopathic pulmonary arterial hypertension (IPAH).^[21]

While CXR can help steer the further diagnostic path, it suffers from limitations [Table 2]. Some of the major limitations are the nonspecific nature of the findings and lack of correlation of disease severity with the extent of radiographic abnormalities. Thus, a normal CXR does not exclude PH. With the availability of newer cross-sectional imaging tools such as computed tomography (CT) and magnetic resonance imaging (MRI), CXR has lost some of its importance although it remains widely used due to ease of availability and lower cost.

Determining Etiology of Pulmonary Hypertension

Computed tomography and computed tomographic pulmonary angiography

CT is gaining acceptance as one of the frontline tests for the evaluation of PH. Fast scanning, excellent spatial and temporal resolution, and ability to comprehensively evaluate the cardiopulmonary structures are some of the distinct advantages that CT offers. With respect to PH, CT plays a modest role in the diagnosis of PH. A major role of CT is in assessment of the cause of PH. CT allows comprehensive evaluation of the pulmonary vasculature and lung parenchyma. In addition, cardiovascular changes secondary to PH can be well assessed with CT, which allows evaluation of severity of the disease.

Computed tomography angiography protocol

At our institution, several different scanners are available including the second generation dual-source scanners (Siemens SOMATOM FLASH; Siemens Healthcare, Germany). A good proportion of the patients referred for CT have a known diagnosis of PH, and a routine non-electrocardiogram (ECG)-gated contrast-enhanced CT is performed for the evaluation of PA and lung parenchyma. If there is clinical concern for PE and if detailed evaluation of cardiovascular structures is desired, an ECG-gated computed tomography angiography (CTA) is performed. ECG gating improves assessment of RV parameters such as enlargement and hypertrophy.^[22] Furthermore, a novel, high-pitch ECG-synchronized computed tomographic pulmonary

angiography (CTPA) protocol can be used to allow better contrast opacification of the pulmonary vasculature at reduced radiation dose.^[23]

Lung parenchyma

CT can reveal abnormalities in the lung parenchyma of PH patients. Chronic, progressive processes such as emphysema and idiopathic pulmonary fibrosis have characteristic CT findings.^[24] In addition, patients with PAH may experience episodes of pulmonary hemorrhage. Pulmonary macrophages ingest these red blood cells, forming cholesterol granulomas that are visualized as centrilobular ground-glass nodules on CT.^[25] Centrilobular nodules, ground-glass opacities, smooth thickening of the interlobular septa, enlarged mediastinal lymph nodes, and pleural effusions can be seen in pulmonary veno-occlusive disease (PVOD).^[26,27] Extensive and larger ground-glass opacities may support the diagnosis of pulmonary capillary hemangiomatosis (PCH).^[28] The presence of esophageal dilation may hint to limited scleroderma as the cause of PAH.

In patients with CTEPH, one can see peripheral parenchymal opacities (caused by recurring thromboembolic infarctions) and mosaic lung attenuation (alternating regions of oligemia and hyperemia).^[24] The latter describes heterogeneous lung perfusion with sharply demarcated regions of hypoattenuation caused by hypoperfusion in areas distal to occluded vessels or small-vessel arteriopathy.^[24]

Vascular structures

Clinician recognition of dilated PA, its differential diagnosis, and predictive value is imperative.^[7] Persistently high PA pressures cause vascular remodeling, which leads to PA wall thickening and dilation [Figure 3]. The Framingham Heart Study provides the largest cohort ($n = 706$) used to define normal PA size reference ranges.^[29] Investigators reviewed noncontrast chest CTs of this "healthy" cohort (nonsmoker patients without obesity, hypertension, chronic obstructive pulmonary disease, history of PE, diabetes, cardiovascular disease, of heart valve surgery). The mean \pm standard deviation (SD) main PA diameter was 25.1 ± 2.8 mm, and the sex-specific 90th percentile cutoff value for main PA diameter was 28.9 mm in men and 26.9 mm in women. The diameter of the main PA was associated with increased risk for self-reported dyspnea (adjusted odds ratio, 1.31; $P = 0.02$).^[29] Other studies of normative reference ranges for PA size are varied, given differences in measuring methodology (the entire vessel diameter versus the vascular lumen), use of intravenous (IV) contrast, window settings, ECG-gated examinations, underlying medical conditions, and demographics.^[7]

The differential diagnosis for a dilated PA on CTPA is broad. Etiologies include PH and its various etiologies, increased or turbulent blood flow (i.e., left-to-right shunt, patent ductus arteriosus, atrial or ventricular septal defect), rheumatologic diseases (i.e., Behçet disease, Takayasu arteritis), connective tissue diseases (i.e., Marfan syndrome, Ehlers–Danlos syndrome, cystic medial necrosis), infections (i.e., tuberculosis, syphilis), trauma, or idiopathic causes.^[7]

The sensitivity and specificity for detecting PH vary based on the type of PH and PA diameter cutoff used. A systematic

Table 2: Relative strengths and limitations of imaging techniques

	CXR	Echo	CTA	CMRI	V/Q scan	Pulmonary angiogram	DECT	SPECT-CT V/Q
Initial diagnosis	+	++ (often suggests PH)	+	+	-	-	+	-
Assessment of etiology	++	++	+++	+	++	++	++	++
Lung parenchyma	+	-	+++	+	-	-	+++	++
Cardiovascular	+	++	++ (especially on ECG-gated examination)	+++	-	-	++	-
Pulmonary vasculature	+	+	+++	++	+	++ (good for defining anatomy)	+++ (PBV maps can help differentiate large-vessel versus small-vessel diseases)	+
General strengths	Readily available as a screening tool	Good for initial assessment of PH; readily available	Excellent for evaluation of etiologies of PH	No radiation Very good for assessment of cardiovascular function	Good for initial screening of thromboembolic disease	Good for defining anatomy	Allows assessment of anatomy and function in a single test	Allows limited assessment of lung parenchyma (if CT combined) with lung perfusion
Weaknesses	Disease severity does not correlate with changes seen on CXR	Limited role for the assessment of etiology	Radiation risks Limited assessment of hemodynamic assessment	Poor evaluation of lung parenchyma; technically demanding and needs technical expertise	Findings often nonspecific; need further imaging to assess cause; high number of nondiagnostic scans	Radiation risk; fallen out of favor due to rise of CT/MRI; Invasive test	Needs more validation	Lung assessment limited; needs more validation; radiation dose added with use of CT

+ = Limited use; ++ = Moderately useful; +++ = Very useful; RHC = Right heart catheterization; DECT = Dual-energy computed tomography; MRI = Magnetic resonance imaging; RV = Right ventricle; CMRI = Cardiac magnetic resonance imaging; V/Q = Ventilation/perfusion; CT = Computed tomography; SPECT = Single-photon emission computed tomography; PH = Pulmonary hypertension; ECG = Electrocardiogram; CXR = Chest X-ray; CTA = Computed tomography angiography; PBV = Perfusion blood volume

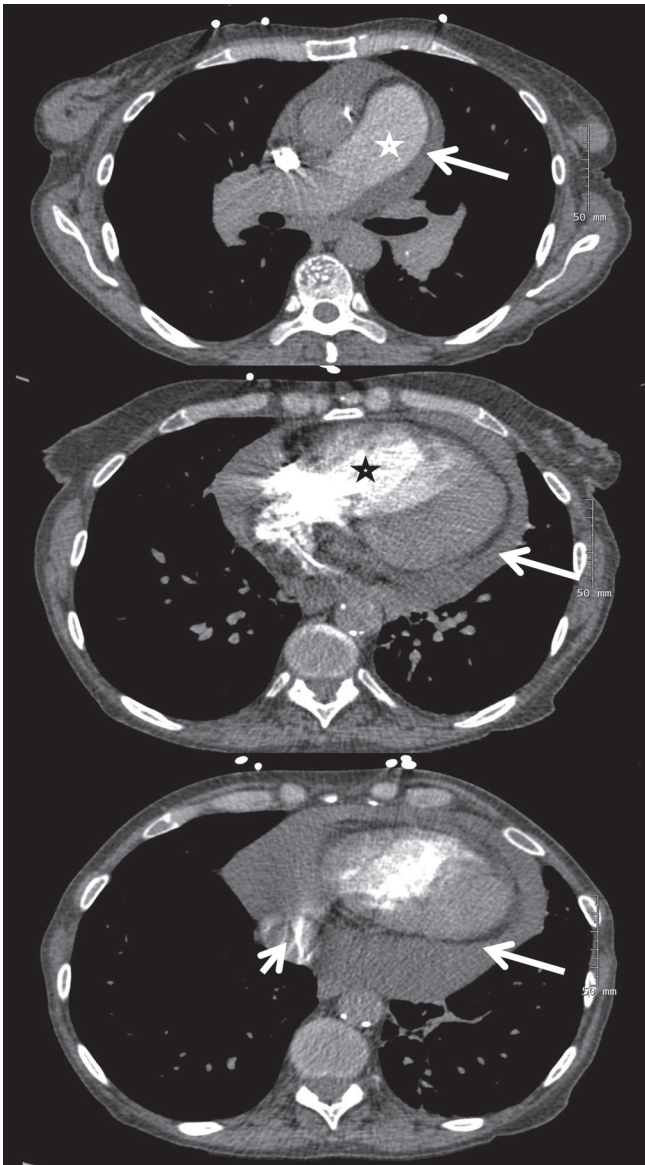


Figure 3: Computed tomographic pulmonary angiography in a patient with idiopathic pulmonary arterial hypertension. Upper panel shows dilated pulmonary artery (star) and pericardial effusion (arrow). Center panel reveals a dilated right ventricle (star) with displacement of the interventricular septum toward the left ventricle and pericardial effusion (arrow). Lower panel shows iodine contrast in the inferior vena cava (short arrow) and pericardial effusion (long arrow)

review of the sensitivity and specificity of different PA diameter cutoffs for identifying PH found an average reported cutoff of 29.5 mm (range 25.0–33.2) among 12 studies that included patients from different PH groups.^[7] Average sensitivity and specificity for detecting PH was 71.9% (range 47%–87%) and 81.1% (range 41%–100%), respectively.^[7] In fact, a dilated PA with a mean diameter ≥ 29 mm has 87% sensitivity and 89% specificity for detecting patients with PH; hence, this cutoff point is often utilized in the literature.^[7,15,25] However, it should be noted that even a normal PA diameter does not exclude PH.^[25]

Specificity of a dilated PA approaches 100% when the segmental artery-to-bronchus ratio is $>1:1$ in 3 of 4 pulmonary

lobes on axial CT images.^[15] A ratio of CT-measured main PA transverse diameter to ascending aorta diameter >1 is also highly indicative of PH, with 96% positive predictive value.^[15] Several studies have suggested a strong association between the ratio of main PA to ascending aortic diameter and PA pressure (in the absence of ectasia or ascending aneurysm of the ascending aorta).^[30–32] The Framingham Heart Study found that the normal mean \pm SD ratio of PA to ascending aorta diameter was 0.77 ± 0.09 , with a 90th percentile cutoff value of 0.91.^[29] The ratio of PA to ascending aorta diameter appears to be a better predictor of mean PA pressure than main PA diameter alone or the ratio of main PA diameter over body surface area.^[33] In fact, Devaraj *et al.* found that PA to ascending aorta ratio significantly correlated with RHC-derived mPAP ($R^2 = 0.45$, $P < 0.001$), an association that was enhanced using RV systolic pressure estimated by echocardiography, yielding a sensitivity of 59% and a specificity of 96% to detect PH.^[34] Nevertheless, practitioners should be wary that clinically significant disease may still be present despite a normal PA: Aorta ratio.

Reduced PA distensibility (the percentage change in cross-sectional area between diastole and systole) measured by ECG-gated CTPA is also another marker of PH: One study proposed $\leq 16.5\%$ as the cutoff for defining PH with a sensitivity of 86% and a specificity of 96%.^[35] Other notable vascular findings on CTPA in patients with Group 1 PH include rapid tapering of the peripheral pulmonary arteries and “corkscrew-like” vessels.^[36]

Vascular patterns may differ according to PH etiology. Typically with IPAH, there is symmetric enlargement of the PA. With CTEPH, there is more irregular dilation of PA with thrombi, which may be calcified. Bronchial artery collaterals can be seen with both IPAH and CTEPH although they are more common with CTEPH.^[37] CT evaluates the presence of other disease processes, such as *in situ* thrombosis that is seen with Eisenmenger syndrome or vasculitides, anomalous pulmonary venous return, large atrial septal defects or other shunts, and miscellaneous conditions such as fibrosing mediastinitis in which the vessels are compressed by an extrinsic process.

CTPA is also important in the assessment of patients with CTEPH being considered for surgical candidacy.^[38] In CTEPH, ventilation/perfusion (V/Q) scanning is still considered as the initial imaging test of choice for diagnosis.^[39] However, once the diagnosis of CTEPH is suggested, CTPA is commonly used to assess the extent of disease and the secondary cardiopulmonary changes. Specifically, CTPA allows identification of proximal disease and extent of thrombi; these patients are good candidates for surgery. CTPA can also identify distal obstructions, narrowing of the pulmonary arteries and their branches, and distal stenosis.^[40] Other findings include pouch-like defects, intimal irregularities, PA webs or bands, as well as enlargement of bronchial arteries due to collateral blood supply.^[41] The presence of bronchial artery collaterals also has prognostic significance in patients with CTEPH since these patients tend to do well postoperatively.^[42]

A dilated PA poses the risk of significant morbidity and mortality, particularly due to compression of critical mediastinal structures. Recognition of the compression of anatomic structures due to PH is imperative as early diagnosis

and aggressive treatment is crucial. Elevated PA pressure and PA size may result in extrinsic compression of the left main coronary artery and subsequent left ventricular (LV) ischemia.^[43,44] A PA diameter >4 cm and a PA to aorta ratio >1.21 pose higher risk of left main coronary artery compression and subsequent complications.^[45] CTPA can suggest this diagnosis, but ideally coronary angiography with intravascular ultrasound is needed for confirmation.^[43,46]

An enlarged PA can compress the left recurrent laryngeal nerve, resulting in cardiovocal (Ortner's) syndrome, characterized by vocal cord palsy and hoarseness. CT or MRI of the head and neck may aid in locating the site of left recurrent laryngeal nerve compression, but definitive diagnosis requires laryngoscopy. Finally, a dilated PA can compress the tracheobronchial tree.^[44] The most common site of compression is where the left PA crosses the superior aspect of the left main bronchus.^[44]

Cardiac chambers

CTPA is also useful for assessing cardiac chambers since ECG-gated CTPA can demonstrate signs of RV failure. These include RV hypertrophy, leftward bowing of the interventricular septum [Figure 3], RV dilation (defined as an RV to LV diameter ratio >1:1 at the mid-ventricular level), dilation of the inferior vena cava and hepatic veins, pericardial effusion and suggestion of tricuspid regurgitation (demonstrated by reflux of contrast into the inferior vena cava and hepatic veins).^[25] Of note, in studies such as CT-PE protocol where the rate of contrast injection is fairly rapid, the reflux of contrast in IVC is somewhat less predictive of RV dysfunction [Figure 3].^[47]

In patients with mPAP \geq 30 mmHg, a leftward deviation of the interventricular septum during systole had an 86% sensitivity and 91% specificity for detecting PH.^[48] Increased end-diastolic thickness of the RV free wall (\geq 6 mm), increased RV/LV lumen ratio \geq 1.28, and RV/LV wall ratio \geq 0.32 have also been found to predict PH.^[49] It is also important to recognize partial anomalous pulmonary venous return since this congenital abnormality may be associated with PH, particularly when it involves two pulmonary veins or there are associated congenital heart diseases, such as an atrial septal defect.^[50]

The septal angle, or the angle formed between the interventricular septum and the line connecting the sternum midpoint and thoracic vertebral spinous process, can also be measured with CTPA. Septal angle is increased in patients with PH and is a typically a sign of right ventricular overload. Prior studies found septal angle measurements to be useful in predicting PVR and strongly correlated with N-terminal pro-B-type natriuretic peptide in patients with CTEPH.^[51,52] Septal angle has also been suggested as a predictor of right ventricular dysfunction in patients with saddle pulmonary embolus.^[53] Nevertheless, further studies are required to clearly define the role of septal angle in diagnosis and assessment of severity of PH.

Like all imaging modalities, CT is not without limitations [Table 2]. PA size on CTA is a poor predictor of PH. CT also provides limited hemodynamic information, especially on non-ECG-gated examinations. CT also exposes patients to radiation, which is especially concerning in patients who undergo repeated examinations.

Ventilation perfusion scan

V/Q scan is the imaging modality of choice for screening patients with suspected CTEPH, due to its high sensitivity [Figure 4].^[2] Imaging in CTEPH reveals wedge-shaped perfusion defects with normal ventilation; meanwhile, complete absence of perfusion to one lung may indicate other conditions such as malignancy, vasculitis, and fibrosing mediastinitis.^[54] A normal- or low-probability V/Q scan effectively excludes CTEPH with a sensitivity of 90%–100% and a specificity of 94%–100%, compared to CTPA which yields a sensitivity of 50%–98% with similar specificity.^[2,39] The V/Q scan also has a higher sensitivity compared to CTPA in detecting distal forms of disease.^[54] A normal perfusion scan or evidence of small peripheral unmatched and nonsegmental defects is commonly seen in PAH.^[54] In the adequate setting, the presence of one or more segmental mismatched perfusion defects warrants further evaluation, i.e., pulmonary angiogram.

Unmatched perfusion defects can manifest in other pulmonary vascular diseases, such as PVOD and PCH. It is crucial to recognize these entities because patients with PVOD and PCH may develop pulmonary edema when treated with pulmonary vasodilator agents.^[55]

Despite the high sensitivity of the V/Q scan in detecting CTEPH and the recommendation to be obtained as part of the diagnostic workup of PH patients, it is underutilized. High-resolution CT of the lungs is often used instead, in part because it is more readily available.^[2] Analysis of a PH registry revealed that 43% of patients diagnosed with PAH never received a V/Q scan.^[56]

Shortcomings of the V/Q scan [Table 2] include its potential for underestimating the extent of central vascular obstruction and its inability to differentiate between similarly presenting diseases such as PVOD and fibrosing mediastinitis.^[53,56,57] Other disadvantages include the high number of nondiagnostic or indeterminate scans and the necessity for further evaluation with cross-sectional imaging to confirm vascular and lung findings and assess the extent of anatomic disease. However, V/Q scans are advantageous in that they do not require iodine contrast and have less radiation exposure than CTPA; the estimated effective dose for thoracic imaging with V/Q is 0.6–3 mSV, whereas for 16-array or greater multi-detector CT, it is 8–20 mSV.^[58] V/Q

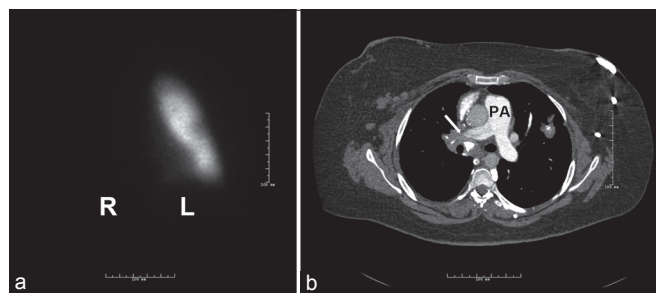


Figure 4: Ventilation perfusion scan and computed tomography angiography in a patient with pulmonary hypertension due to fibrosing mediastinitis and absent flow to the right lung. (a) The lack of perfusion on the right lung. (b) An obstruction of the right main pulmonary artery (white arrow) due to fibrosing mediastinitis. Note the calcified adenopathies and fibrotic tissue. L = left lung, PA = pulmonary artery, R = right lung

is most useful as an effective screening tool in CTEPH as a negative V/Q scan virtually rules out CTEPH.

Cardiac magnetic resonance imaging

While cardiac magnetic resonance (CMR) remains underutilized, it may overcome some of the major limitations of TTE in the assessment of the RV. A wide range of sequences can provide comprehensive structural and functional information in these patients. Cardiac magnetic resonance imaging (CMRI) is safe and does not expose patients to ionizing radiation; however, it is expensive, not widely available, and requires operator expertise [Table 2].

Cardiac magnetic resonance imaging protocol

At our institution, after the initial acquisition of localizer scouts, we obtain axial stack of half-Fourier single-shot echo and steady-state free precession (SSFP) images. Next, we proceed to cine imaging. Typically, a four-chambered cine SSFP stack is obtained to evaluate RV function. These images are usually obtained at 8-mm slice intervals with a 2-mm inter-slice gap. Alternatively, a short-axis stack can be obtained. Next, phase-contrast-MRI (PC-MRI) of the main, right, and left main PA is obtained allowing assessment of peak velocities and differential flow to the right and left lungs. Finally, contrast-enhanced magnetic resonance angiography (MRA) is performed. At our institution, fluoroscopically triggered time-resolved three-dimensional (3D) spoiled gradient echo sequence with view sharing is used. In patients for whom gadolinium is contraindicated, noncontrast MRA techniques such as navigator-gated whole-heart SSFP MRA can be used. However, these techniques are suboptimal for the evaluation of distal segmental and subsegmental vasculature.

CMRI is the current reference standard for the assessment of RV volumes and function,^[59] given the clear “definition” of the interface contour between the blood-myocardium interface and reproducible assessment of RV volume, mass, and function [Figure 5].^[25] Compared to TTE, MRI offers better spatial resolution and is not limited by acoustic windows. Axial views of the cardiac chambers reveal a change in RV morphology from its normal crescent shape to a more round contour due to concentric hypertrophy. Other abnormalities seen in PH include RV wall motion abnormalities, reduced RV ejection fraction, RV hypertrophy (due to chronic pressure overload), RV dilation, flattening or leftward bowing of the interventricular septum, RA enlargement, and tricuspid regurgitation [Figures 5 and 6].^[60,61] ECG-gated cine images can quantify RV chamber size and systolic function; reduced stroke volume on CMRI has been linked with increased mortality.^[62] LV abnormalities are also commonly noted such as reduced LV end-diastolic volume and stroke volume^[61] [Video 1].

Interventricular septal bowing is indicative of a systolic pulmonary arterial pressure (sPAP) ≥ 67 mmHg and leads to impaired filling in early diastole and decreased LV stroke volume [Figure 6].^[48] Thus, the degree of left septal bowing is of prognostic value.^[63] In addition, RV mass is greater in PH compared to healthy controls; a ventricular mass index (RV mass divided by LV mass) >0.6 is indicative of PH (sensitivity 84% and specificity 71%).^[25] Studies have reported varying positive correlations between ventricular mass index and mPAP (range 0.56–0.81).^[25] PA pulsatility of

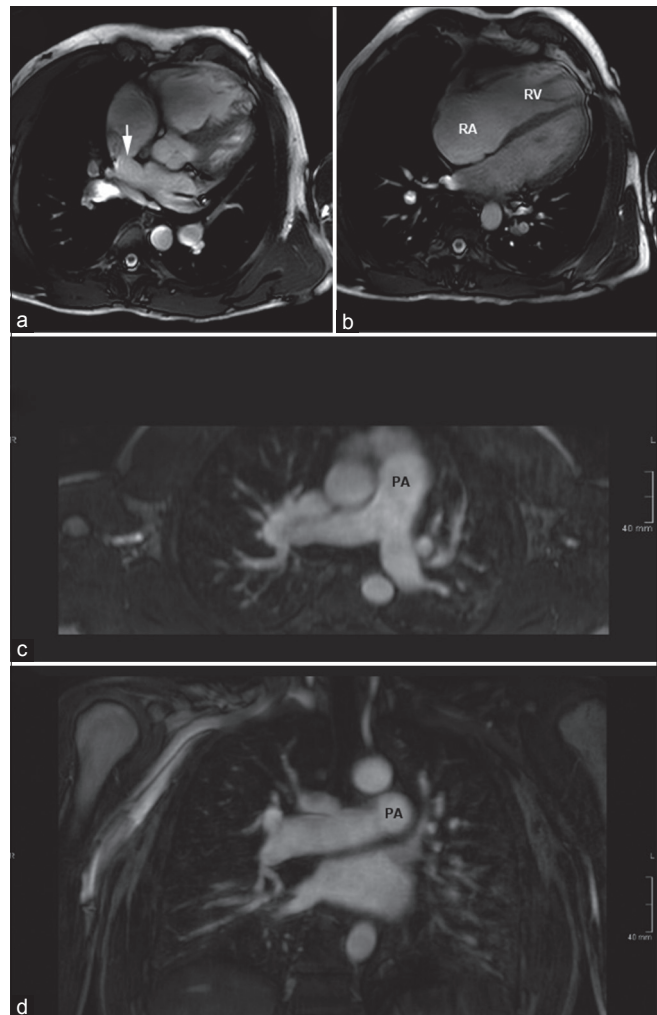


Figure 5: Magnetic resonance imaging in a patient with sinus venosus atrial septal defect and partial anomalous pulmonary venous return. (a and b) Images from a steady state free precession cine 4-chambered stack show the superior sinus venosus defect (arrow). There is severe dilation of the right-sided chambers. (c and d) Reconstructed images from magnetic resonance angiography show dilation of the central pulmonary arteries. The patient had a significant left-to-right shunt with Qp/Qs of 3.6. RV = Right ventricle, RA = right atrium, PA = Pulmonary artery

deformation is another useful measure obtained with CMRI and can indicate increased PA stiffness and increased risk of mortality.^[62] Noninvasive assessment of PVR is ideal in this patient population for the assessment of response to therapy and follow-up.^[64]

While CMRI is a valuable tool in characterizing patients with PH, RHC remains the gold standard for diagnosis; furthermore, no single CMRI measurement can exclude PH. Rather, CMRI provides valuable information regarding response to the treatment. CMRI assessment of PA distensibility correlates well with response to vasodilator therapy, with a cutoff of 10% (sensitivity 100% and specificity 56%).^[65] In fact, proximal PA stiffness has been shown to predict mortality in patients with PH.^[66] Furthermore, a CMR study of 64 patients with IPAH found that large RV volume and low stroke volume at baseline were strong independent predictors of mortality and treatment failure.^[67] RV failure is the most common cause of death in PH patients;^[7] therefore, it has been suggested that

serial CMRIs may be adequate to monitor treatment response and prognosis.^[25]

Phase contrast imaging

Phase-contrast is an MRI technique used to measure vascular velocity and blood flow; therefore, it provides an assessment of cardiac output, RV stroke volume, and cardiac shunts. PH patients may demonstrate decreased mean flow velocity in the PA, with one study reporting mean velocity in the PA to be <11.7 cm/s (sensitivity 92.9% and specificity 82.4%) in PH patients.^[68] PC-MRI can also evaluate coronary perfusion of the RV and determine the presence of RV ischemia, which leads to RV failure in PH.^[62] One study of PAH patients found that right coronary artery peak and mean systolic flow was significantly decreased compared to control patients; these changes were inversely correlated to RV mass and RV pressure.^[69] PC-MRI has also been used to determine advanced hemodynamic parameters such as pulse-wave velocity, vorticity, and wall shear stress.^[62]

Delayed enhancement-cardiac magnetic resonance imaging

Imaging performed 10–15 min after receiving IV gadolinium permits visualization of myocardial scarring, which is seen as delayed contrast enhancement at RV septal insertion points at the base of the heart.^[70,71] This signifies increased mechanical stress due to chronically high RV pressures and is correlated with poorer RV function and hemodynamics.

While CMR has the capability to become the “one stop shop” imaging tool in evaluation of PH, its utilization has still been limited [Table 2]. One of the major limitations of CMR remains the limited evaluation of lung parenchyma. While newer techniques such as ultra-short echo time imaging show promise, these are still in early stages of development.^[72] Other limitations of CMR include longer scan times and high technical demands.

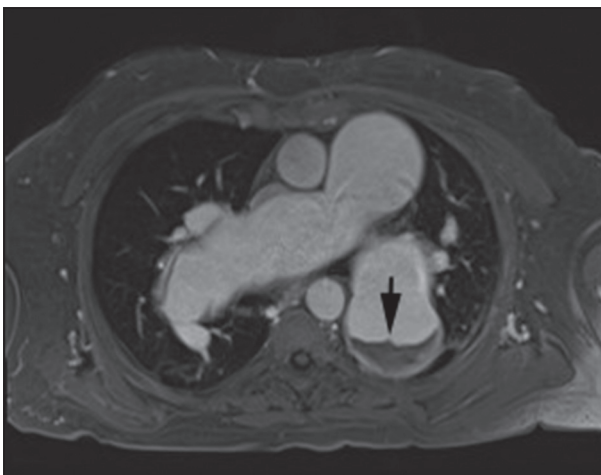


Figure 6: Magnetic resonance imaging in a 67 male patient with long-standing severe pulmonary hypertension. Axial postgadolinium VIBE (volume interpolated breath-hold) image shows aneurysmal pulmonary arteries with layered *in situ* thrombus in left lower lobar pulmonary artery (arrow). Cine steady-state free precession 4-chamber supplementary video clip shows massively enlarged bilateral pulmonary arteries with layered *in situ* thrombus. There is associated right ventricle enlargement and right ventricular hypertrophy. The right ventricle systolic function was moderately depressed (ejection fraction-40%). Cine steady-state free precession nicely depicts the swirling of blood within the pulmonary arteries, reflecting sluggish flow. Also seen is mild tricuspid regurgitation

Other Imaging Modalities

Abdominal ultrasound

Abdominal ultrasound can identify clinical conditions associated with PH, such as liver cirrhosis and portal hypertension. The latter is confirmed with an increased gradient between the free and occluded hepatic vein pressure at RHC.^[73] Mild splenomegaly has also been found to be common in patients with idiopathic and heritable PAH.^[74]

Pulmonary angiogram

Although the value of pulmonary angiogram has diminished with the increasing utilization of CT/MRI, it is still used to define the extent of disease in CTEPH [Figure 7]. Findings seen on pulmonary angiogram are similar to those of CTA although the wall changes are suboptimally evaluated. In addition, pulmonary angiogram allows good qualitative assessment of lung perfusion in these patients. The success of interventional techniques such as balloon angioplasty in treatment of CTEPH might lead to renewed interest in this technique.

Novel Imaging Modalities

Single-photon emission computed tomography/computed tomography

Single-photon emission computed tomography/computed tomography (SPECT/CT) is a relatively novel nuclear medicine imaging study that integrates CT and a gamma camera to provide both anatomical data from CT and functional information from SPECT [Figure 8].^[75] SPECT/CT evaluates regional lung perfusion and can generate 3D fusion images to visualize PA structures and segmental lung perfusion, allowing rapid identification of regions of hypoperfusion.^[76] Heretofore, it has chiefly been used to diagnose PE. In a study of 84 patients, SPECT/CT yielded a significantly higher diagnostic accuracy for PE (sensitivity 100% and specificity 83%) than planar and SPECT scans.^[77] More recently, SPECT/CT has been used to evaluate CTEPH.^[78] A study of 15 patients with precapillary PH and 11 healthy controls calculated a perfusion redistribution index (PRI) using SPECT/CT images. This index quantified

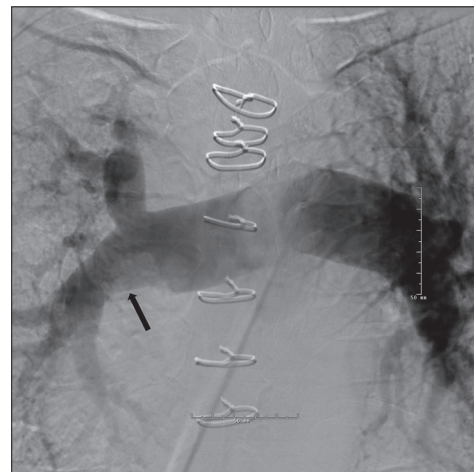


Figure 7: Pulmonary angiogram in a patient with chronic thromboembolic pulmonary hypertension and 50% chronic obstruction of the right main pulmonary artery. The black arrow points toward the narrowing of the right pulmonary artery. Note the diameter difference between the right and left main pulmonary arteries

gravity-dependent shifts in regional lung perfusion as a marker of pulmonary vascular reserve.^[79] Patients with precapillary PH had statistically significant reduced PRI compared to controls, and PRI was associated with a number of prognostic factors.^[79] A study found SPECT perfusion scans to be more sensitive than planar V/Q scans in identifying obstructed segments in CTEPH.^[80] Another study demonstrated that SPECT was more sensitive than CTPA in identifying obstructed vascular segments.^[80]

While SPECT/CT may be highly sensitive, it may underrepresent the true extent of vascular obstruction in CTEPH.^[80] Nevertheless, data regarding the utility of SPECT/CT are insufficient, and its superiority or inferiority to more traditional imaging techniques must further be investigated before it can be properly integrated into clinical practice.

Dual-energy computed tomography

Dual-energy computed tomography (DECT) provides similar vascular and parenchymal findings as conventional CT such

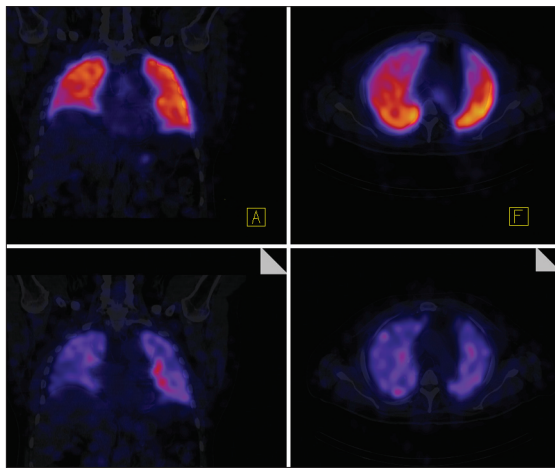


Figure 8: Representative normal SPECT-CT image. The top two panels show perfusion images while bottom two images show ventilation. SPECT-CT allows better mapping of perfusion defects to the appropriate lung segments. SPECT-CT = Single-photon emission computed tomography/computed tomography

as PA diameter and morphology, with the added benefit of perfusion analysis of the lung via iodine maps correlated with scintigraphy.^[81,82] DECT exploits the differences in attenuation of iodine at low and high kilovoltage (typically 80 and 140 kVp). Different vendors approach spectral CT in different ways include the use of two X-ray tubes, rapid kilovoltage switching, and use of energy sensitive detector.^[81] Regardless of the technique, the attenuation spectra at low and high photon energies are used to separate materials such as iodine and calcium. Calculation of amount of iodine in a voxel is used to generate perfused blood volume (PBV) images [Figures 9 and 10]. While these are not strictly perfusion images as they measure iodine at a single time point, they serve as adequate surrogate markers of lung perfusion.^[24] Automated quantification of PBV maps can allow an objective assessment of the relative lung perfusion. Perfusion defects seen with DECT appear to correlate well with V/Q and SPECT V/Q images.^[83] Furthermore, the presence or absence of iodine in a voxel can be used to generate a lung vessel map [Figure 10]. Recent studies have shown added value of DECT and PBV maps in the imaging and risk stratification of patients with acute PE, as well as in the assessment of prognosis.^[84,85] PBV maps allow increased confidence in diagnosis, and automated quantification of PBV maps also assist in prognosis. Currently, pulmonary blood volume imaging and perfusion maps are used to evaluate acute PE since they have been shown to be comparable to V/Q scintigraphy.^[81] In chronic PE, the ability of PBV images to provide perfusion images coupled with anatomic images make it a potential “one stop shop” tool.^[82]

DECT reveals the distribution of central and peripheral vascular perfusion as well as details of pulmonary parenchymal enhancement. It allows mapping of anatomic defects and correlates them with functional information. Thus, vascular anatomy, parenchymal morphology, and functional analysis of the lung can all be obtained in a single test. In CTEPH patients, PBV maps have been used to assess surgical candidacy and pulmonary hemodynamics. One study showed a trend for PBV values to correlate inversely with PVR.^[86]

In addition, delayed phase DECT has been used to differentiate between acute and chronic PE. Typically, perfusion defects

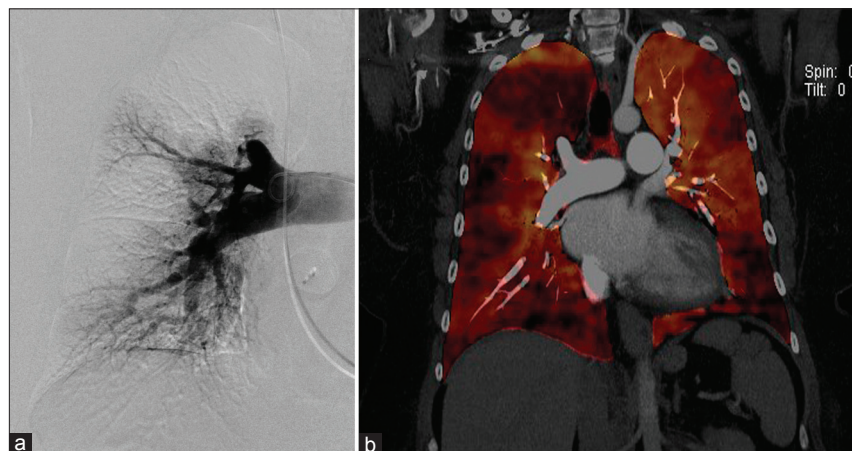


Figure 9: Dual-energy computed tomography in a patient with chronic thromboembolic pulmonary hypertension. (a) Pouch sign on the right upper pulmonary artery on a pulmonary angiogram and corresponding defect on the dual-energy computed tomography image. (b) Fused-perfused blood volume images generated by fusion of the anatomic and perfused blood volume datasets. This allows correlating anatomic and functional information. The pouch defect is again seen with corresponding wedge-shaped perfusion defect

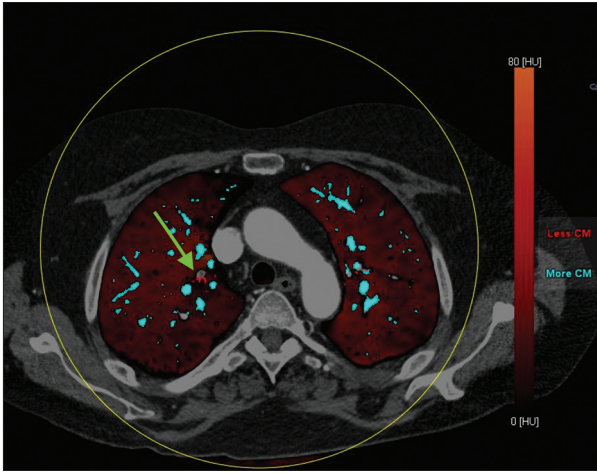


Figure 10: Fused lung vessel and perfused blood volume map image in a patient with acute pulmonary embolism. The vessels containing iodine are coded blue. The subsegmental branch with acute PE is highlighted easily on the lung vessel map, which can be fused on perfused blood volume maps

seen with chronic PE show delayed enhancement due to the presence of collateral supply. In addition, this can serve as an indirect marker of bronchial collateral supply, which can be a good prognostic marker in CTEPH.^[87] DECT-derived PBV may have the potential to elucidate causes of PH; typically, CTEPH will display large perfusion defects, whereas IPAH will display smaller, mottled defects. DECT can also identify PH due to congenital heart disease, particularly in the neonatal population.

Right ventricular mapping magnetic resonance imaging

RV T1 mapping can be used to identify diffuse myocardial abnormalities. T1 mapping values have been associated with indices of RV dysfunction.^[88,89] T1 mapping identifies diffuse interstitial abnormalities in the RV and metrics derived from this modality help recognize ventricular fibrosis. Therefore, RV T1 mapping is a promising modality to detect diffuse myocardial fibrosis in RV failure, an important aspect of PH prognosis. RV T1 mapping may be a useful tool in determining therapeutic response in PH.

Pulmonary artery four-dimensional flow imaging

Proximal PA changes are common in PH. 4D-flow MRI permits noninvasive measurements of complex 3D hemodynamic changes with full volumetric coverage of the RV and PA.^[61] Volumetric analysis utilizing 4D-flow MRI can provide accurate assessment of aortic and PA peak velocities.^[90] 4D-flow MRI has demonstrated abnormal vortex development of the main PA, which correlates with main PA pressure.^[91-93] A recent 4D flow study in a canine model of acute thromboembolic PH quantified RV and LV function, PA flow, tricuspid valve regurgitant velocity, and aorta flow in a single examination.^[94] 4D-flow MRI has shown low interobserver variability, high reliability, and adequate correlation between flow parameters obtained via 4D-flow MRI and 2D-cine PC-MRI.^[95,96] 4D-flow MRI may provide understanding into the various flow changes that occur in PH and enhance our diagnostic and prognostic capability.

Right ventricular strain

RV strain mapping provides quantitative evaluation of regional myocardial function, improving sensitivity of CMR

to regional abnormalities in RV function. Myocardial strain can be calculated with several CMR techniques: Myocardial tagging, harmonic phase analysis, displacement encoding, strain-encoded imaging, deformation field analysis, and multimodality feature tracking.^[62] Strain analysis can be useful for identifying early changes in RV function before reductions in global RV function and ventricular dyssynchrony by myocardial tagging.^[97] This technique is however in early stages, and more studies are needed before integration in clinical practice.

Conclusion

PH can be evaluated with a multitude of imaging techniques. CXR is commonly used in the initial evaluation of PH and can provide information regarding changes in cardiac morphology, underlying lung disease, and loss of peripheral blood vessels. CTPA evaluates vascular structures, cardiac chambers, and lung parenchyma, with PA dilation, ratio of main PA to ascending aorta diameter, PA distensibility, and RV morphologic changes being useful measures. V/Q scan is most useful in identifying CTEPH patients, highlighting unmatched perfusion defects. CMRI provides useful information of RV and LV anatomy and function. Novel imaging techniques such as SPECT and DECT continue to be investigated, and their role in the diagnostic evaluation of PH remains to be elucidated.

Financial support and sponsorship

A.R.T. is supported by NIH grant #R01HL130307.

Conflicts of interest

There are no conflicts of interest.

References

1. Simonneau G, Gatzoulis MA, Adatia I, Celermajer D, Denton C, Ghofrani A, et al. Updated clinical classification of pulmonary hypertension. *J Am Coll Cardiol* 2013;62 25 Suppl: D34-41.
2. Galie` N, Humbert M, Vachiery JL, Gibbs S, Lang I, Torbicki A, et al. 2015 ESC/ERS Guidelines for the diagnosis and treatment of pulmonary hypertension: The Joint Task Force for the Diagnosis and Treatment of Pulmonary Hypertension of the European Society of Cardiology (ESC) and the European Respiratory Society (ERS): Endorsed by: Association for European Paediatric and Congenital Cardiology (AEPC), International Society for Heart and Lung Transplantation (ISHLT). *Eur Heart J* 2016;37:67-119.
3. Hoepfer MM, Bogaard HJ, Condliffe R, Frantz R, Khanna D, Kurzyna M, et al. Definitions and diagnosis of pulmonary hypertension. *J Am Coll Cardiol* 2013;62 25 Suppl: D42-50.
4. McGoon MD, Benza RL, Escribano-Subias P, Jiang X, Miller DP, Peacock AJ, et al. Pulmonary arterial hypertension: Epidemiology and registries. *J Am Coll Cardiol* 2013;62 25 Suppl: D51-9.
5. Farber HW, Miller DP, Poms AD, Badesch DB, Frost AE, Muros-Le Rouzic E, et al. Five-year outcomes of patients enrolled in the REVEAL Registry. *Chest* 2015;148:1043-54.
6. Raymond TE, Khabbaza JE, Yadav R, Tonelli AR. Significance of main pulmonary artery dilation on imaging studies. *Ann Am Thorac Soc* 2014;11:1623-32.
7. Tonelli AR, Arelli V, Minai OA, Newman J, Bair N, Heresi GA, et al. Causes and circumstances of death in pulmonary arterial hypertension. *Am J Respir Crit Care Med* 2013;188:365-9.
8. Ahmed M, Dweik RA, Tonelli AR. What is the best approach to a high systolic pulmonary artery pressure on echocardiography? *Cleve Clin J Med* 2016;83:256-60.

9. Arcasoy SM, Christie JD, Ferrari VA, Sutton MS, Zisman DA, Blumenthal NP, *et al.* Echocardiographic assessment of pulmonary hypertension in patients with advanced lung disease. *Am J Respir Crit Care Med* 2003;167:735-40.
10. Rich S, Dantzker DR, Ayres SM, Bergofsky EH, Brundage BH, Detre KM, *et al.* Primary pulmonary hypertension. A national prospective study. *Ann Intern Med* 1987;107:216-23.
11. Grünig E, Peacock AJ. Imaging the heart in pulmonary hypertension: An update. *Eur Respir Rev* 2015;24:653-64.
12. Baque-Juston MC, Wells AU, Hansell DM. Pericardial thickening or effusion in patients with pulmonary artery hypertension: A CT study. *AJR Am J Roentgenol* 1999;172:361-4.
13. Weissman NJ, Adelman GA. *Cardiac Imaging Secrets*. Philadelphia, Pennsylvania: Elsevier Health Sciences; 2004.
14. Desai S. Cardiac emergencies. In: Stone C, Humphries RL, editors. *CURRENT Diagnosis & Treatment Emergency Medicine*. 7th ed., Ch. 34. New York: McGraw-Hill; 2011. Available from: <http://www.accessmedicine.mhmedical.com/content.aspx?bookid=385&Sectionid=40357250>. [Last accessed on 2016 Jun 06].
15. Frazier AA, Burke AP. The imaging of pulmonary hypertension. *Semin Ultrasound CT MR* 2012;33:535-51.
16. Milne EN. Forgotten gold in diagnosing pulmonary hypertension: The plain chest radiograph. *Radiographics* 2012;32:1085-7.
17. Helmlinger M, Pienn M, Urschler M, Kullnig P, Stollberger R, Kovacs G, *et al.* Quantification of tortuosity and fractal dimension of the lung vessels in pulmonary hypertension patients. *PLoS One* 2014;9:e87515.
18. Hopkins N, McLoughlin P. The structural basis of pulmonary hypertension in chronic lung disease: Remodelling, rarefaction or angiogenesis? *J Anat* 2002;201:335-48.
19. Olufsen MS, Hill NA, Vaughan GD, Sainsbury C, Johnson M. Rarefaction and blood pressure in systemic and pulmonary arteries. *J Fluid Mech* 2012;705:280-305.
20. Yazdani M, Lau CT, Lempel JK, Yadav R, El-Sherief AH, Azok JT, *et al.* Historical evolution of imaging techniques for the evaluation of pulmonary embolism. *Radiographics* 2015;35:1245-62.
21. Satoh T, Kyotani S, Okano Y, Nakanishi N, Kunieda T. Descriptive patterns of severe chronic pulmonary hypertension by chest radiography. *Respir Med* 2005;99:329-36.
22. Abel E, Jankowski A, Pison C, Luc Bosson J, Bouvaist H, Ferretti GR. Pulmonary artery and right ventricle assessment in pulmonary hypertension: Correlation between functional parameters of ECG-gated CT and right-side heart catheterization. *Acta Radiol* 2012;53:720-7.
23. Bolen MA, Renapurkar RD, Popovic ZB, Heresi GA, Flamm SD, Lau CT, *et al.* High-pitch ECG-synchronized pulmonary CT angiography versus standard CT pulmonary angiography: A prospective randomized study. *AJR Am J Roentgenol* 2013;201:971-6.
24. Kreitner KF. Noninvasive imaging of pulmonary hypertension. *Semin Respir Crit Care Med* 2014;35:99-111.
25. Peña E, Dennie C, Veinot J, Muñoz SH. Pulmonary hypertension: How the radiologist can help. *Radiographics* 2012;32:9-32.
26. Mineo G, Attinà D, Mughetti M, Balacchi C, De Luca F, Niro F, *et al.* Pulmonary veno-occlusive disease: The role of CT. *Radiol Med* 2014;119:667-73.
27. Montani D, Lau EM, Dorfmueller P, Girerd B, Jaïs X, Savale L, *et al.* Pulmonary veno-occlusive disease. *Eur Respir J* 2016;47:1518-34.
28. Miura A, Akagi S, Nakamura K, Ohta-Ogo K, Hashimoto K, Nagase S, *et al.* Different sizes of centrilobular ground-glass opacities in chest high-resolution computed tomography of patients with pulmonary veno-occlusive disease and patients with pulmonary capillary hemangiomatosis. *Cardiovasc Pathol* 2013;22:287-93.
29. Truong QA, Massaro JM, Rogers IS, Mahabadi AA, Kriegel MF, Fox CS, *et al.* Reference values for normal pulmonary artery dimensions by noncontrast cardiac computed tomography: The Framingham Heart Study. *Circ Cardiovasc Imaging* 2012;5:147-54.
30. Kuriyama K, Gamsu G, Stern RG, Cann CE, Herfkens RJ, Brundage BH. CT-determined pulmonary artery diameters in predicting pulmonary hypertension. *Invest Radiol* 1984;19:16-22.
31. Mahammedi A, Oshmyansky A, Hassoun PM, Thiemann DR, Siegelman SS. Pulmonary artery measurements in pulmonary hypertension: The role of computed tomography. *J Thorac Imaging* 2013;28:96-103.
32. Bouchard A, Higgins CB, Byrd BF 3rd, Amparo EG, Osaki L, Axelrod R. Magnetic resonance imaging in pulmonary arterial hypertension. *Am J Cardiol* 1985;56:938-42.
33. Murray TI, Boxt LM, Katz J, Reagan K, Barst RJ. Estimation of pulmonary artery pressure in patients with primary pulmonary hypertension by quantitative analysis of magnetic resonance images. *J Thorac Imaging* 1994;9:198-204.
34. Devaraj A, Wells AU, Meister MG, Corte TJ, Wort SJ, Hansell DM. Detection of pulmonary hypertension with multidetector CT and echocardiography alone and in combination. *Radiology* 2010;254:609-16.
35. Revel MP, Faivre JB, Remy-Jardin M, Delannoy-Deken V, Duhamel A, Remy J. Pulmonary hypertension: ECG-gated 64-section CT angiographic evaluation of new functional parameters as diagnostic criteria. *Radiology* 2009;250:558-66.
36. Junqueira FP, Lima CM, Coutinho AC Jr., Parente DB, Bittencourt LK, Bessa LG, *et al.* Pulmonary arterial hypertension: An imaging review comparing MR pulmonary angiography and perfusion with multidetector CT angiography. *Br J Radiol* 2012;85:1446-56.
37. Remy-Jardin M, Duhamel A, Deken V, Bouaziz N, Dumont P, Remy J. Systemic collateral supply in patients with chronic thromboembolic and primary pulmonary hypertension: Assessment with multi-detector row helical CT angiography. *Radiology* 2005;235:274-81.
38. Fedullo PF, Auger WR, Kerr KM, Rubin LJ. Chronic thromboembolic pulmonary hypertension. *N Engl J Med* 2001;345:1465-72.
39. Tunariu N, Gibbs SJ, Win Z, Gin-Sing W, Graham A, Gishen P, *et al.* Ventilation-perfusion scintigraphy is more sensitive than multidetector CTPA in detecting chronic thromboembolic pulmonary disease as a treatable cause of pulmonary hypertension. *J Nucl Med* 2007;48:680-4.
40. Tonelli AR, Ahmed M, Hamed F, Prieto LR. Peripheral pulmonary artery stenosis as a cause of pulmonary hypertension in adults. *Pulm Circ* 2015;5:204-10.
41. Auger WR, Kerr KM, Kim NH, Fedullo PF. Evaluation of patients with chronic thromboembolic pulmonary hypertension for pulmonary endarterectomy. *Pulm Circ* 2012;2:155-62.
42. Kauczor HU, Schwickert HC, Mayer E, Schweden F, Schild HH, Thelen M. Spiral CT of bronchial arteries in chronic thromboembolism. *J Comput Assist Tomogr* 1994;18:855-61.
43. Kawut SM, Silvestry FE, Ferrari VA, DeNofrio D, Axel L, Loh E, *et al.* Extrinsic compression of the left main coronary artery by the pulmonary artery in patients with long-standing pulmonary hypertension. *Am J Cardiol* 1999;83:984-6, A10.
44. Dakkak W, Tonelli AR. Compression of adjacent anatomical structures by pulmonary artery dilation. *Postgrad Med* 2016;128:451-9.
45. Mesquita SM, Castro CR, Ikari NM, Oliveira SA, Lopes AA. Likelihood of left main coronary artery compression based on pulmonary trunk diameter in patients with pulmonary hypertension. *Am J Med* 2004;116:369-74.
46. Demkow M, Kalinczuk L, Kepka C, Kurzyna M, Torbicki A. Left main artery compression by pulmonary artery aneurysm and ostial athero-stenosis of left anterior descending artery in a young female with pulmonary arterial hypertension. *Eur Heart J* 2012;33:2621.
47. Yeh BM, Kurzman P, Foster E, Qayyum A, Joe B, Coakley F. Clinical relevance of retrograde inferior vena cava or hepatic vein

- opacification during contrast-enhanced CT. *AJR Am J Roentgenol* 2004;183:1227-32.
48. Alunni JP, Degano B, Arnaud C, Tétu L, Blot-Soulétie N, Didier A, et al. Cardiac MRI in pulmonary artery hypertension: Correlations between morphological and functional parameters and invasive measurements. *Eur Radiol* 2010;20:1149-59.
 49. Chan AL, Juarez MM, Shelton DK, MacDonald T, Li CS, Lin TC, et al. Novel computed tomographic chest metrics to detect pulmonary hypertension. *BMC Med Imaging* 2011;11:7.
 50. Sahay S, Krasuski RA, Tonelli AR. Partial anomalous pulmonary venous connection and pulmonary arterial hypertension. *Respirology* 2012;17:957-63.
 51. Tang Q, Liu M, Ma Z, Guo X, Kuang T, Yang Y. Non-invasive evaluation of hemodynamics in pulmonary hypertension by a septal angle measured by computed tomography pulmonary angiography: Comparison with right-heart catheterization and association with N-terminal pro-B-type natriuretic peptide. *Exp Ther Med* 2013;6:1350-8.
 52. Liu M, Ma ZH, Guo XJ, Wang SK, Chen XY, Yang YH, et al. A septal angle measured on computed tomographic pulmonary angiography can noninvasively estimate pulmonary vascular resistance in patients with chronic thromboembolic pulmonary hypertension. *J Thorac Imaging* 2012;27:325-30.
 53. Liu M, Miao R, Guo X, Zhu L, Zhang H, Hou Q, et al. Saddle pulmonary embolism: Laboratory and computed tomographic pulmonary angiographic findings to predict short-term mortality. *Heart Lung Circ* 2016. pii: S1443-950630038-5.
 54. D'Armini AM. Diagnostic advances and opportunities in chronic thromboembolic pulmonary hypertension. *Eur Respir Rev* 2015;24:253-62.
 55. Resten A, Maître S, Humbert M, Sitbon O, Capron F, Simoneau G, et al. Pulmonary arterial hypertension: Thin-section CT predictors of epoprostenol therapy failure. *Radiology* 2002;222:782-8.
 56. McLaughlin VV, Langer A, Tan M, Clements PJ, Oudiz RJ, Tapson VF, et al. Contemporary trends in the diagnosis and management of pulmonary arterial hypertension: An initiative to close the care gap. *Chest* 2013;143:324-32.
 57. Jenkins D, Mayer E, Screaton N, Madani M. State-of-the-art chronic thromboembolic pulmonary hypertension diagnosis and management. *Eur Respir Rev* 2012;21:32-9.
 58. Schembri GP, Miller AE, Smart R. Radiation dosimetry and safety issues in the investigation of pulmonary embolism. *Semin Nucl Med* 2010;40:442-54.
 59. Lorenz CH, Walker ES, Morgan VL, Klein SS, Graham TP Jr. Normal human right and left ventricular mass, systolic function, and gender differences by cine magnetic resonance imaging. *J Cardiovasc Magn Reson* 1999;1:7-21.
 60. Frank H, Globits S, Glogar D, Neuhold A, Kneussl M, Mlczoch J. Detection and quantification of pulmonary artery hypertension with MR imaging: Results in 23 patients. *AJR Am J Roentgenol* 1993;161:27-31.
 61. McLure LE, Peacock AJ. Cardiac magnetic resonance imaging for the assessment of the heart and pulmonary circulation in pulmonary hypertension. *Eur Respir J* 2009;33:1454-66.
 62. Freed BH, Collins JD, François CJ, Barker AJ, Cuttica MJ, Chesler NC, et al. MR and CT imaging for the evaluation of pulmonary hypertension. *JACC Cardiovasc Imaging* 2016;9:715-32.
 63. D'Alonzo GE, Barst RJ, Ayres SM, Bergofsky EH, Brundage BH, Detre KM, et al. Survival in patients with primary pulmonary hypertension. Results from a national prospective registry. *Ann Intern Med* 1991;115:343-9.
 64. Kreitner KF, Wirth GM, Krummenauer F, Weber S, Pitton MB, Schneider J, et al. Noninvasive assessment of pulmonary hemodynamics in patients with chronic thromboembolic pulmonary hypertension by high temporal resolution phase-contrast MRI: Correlation with simultaneous invasive pressure recordings. *Circ Cardiovasc Imaging* 2013;6:722-9.
 65. Jardim C, Rochitte CE, Humbert M, Rubinfeld G, Jasinowodolinski D, Carvalho CR, et al. Pulmonary artery distensibility in pulmonary arterial hypertension: An MRI pilot study. *Eur Respir J* 2007;29:476-81.
 66. Gan CT, Lankhaar JW, Westerhof N, Marcus JT, Becker A, Twisk JW, et al. Noninvasively assessed pulmonary artery stiffness predicts mortality in pulmonary arterial hypertension. *Chest* 2007;132:1906-12.
 67. van Wolferen SA, Marcus JT, Boonstra A, Marques KM, Bronzwaer JG, Spreeuwenberg MD, et al. Prognostic value of right ventricular mass, volume, and function in idiopathic pulmonary arterial hypertension. *Eur Heart J* 2007;28:1250-7.
 68. Sanz J, Kuschner P, Rius T, Salguero R, Sulica R, Einstein AJ, et al. Pulmonary arterial hypertension: Noninvasive detection with phase-contrast MR imaging. *Radiology* 2007;243:70-9.
 69. van Wolferen SA, Marcus JT, Westerhof N, Spreeuwenberg MD, Marques KM, Bronzwaer JG, et al. Right coronary artery flow impairment in patients with pulmonary hypertension. *Eur Heart J* 2008;29:120-7.
 70. Blyth KG, Groenning BA, Martin TN, Foster JE, Mark PB, Dargie HJ, et al. Contrast enhanced-cardiovascular magnetic resonance imaging in patients with pulmonary hypertension. *Eur Heart J* 2005;26:1993-9.
 71. McCann GP, Gan CT, Beek AM, Niessen HW, VonkNoordegraaf A, van Rossum AC. Extent of MRI delayed enhancement of myocardial mass is related to right ventricular dysfunction in pulmonary artery hypertension. *AJR Am J Roentgenol* 2007;188:349-55.
 72. Ohno Y, Koyama H, Yoshikawa T, Seki S, Takenaka D, Yui M, et al. Pulmonary high-resolution ultrashort TE MR imaging: Comparison with thin-section standard- and low-dose computed tomography for the assessment of pulmonary parenchyma diseases. *J Magn Reson Imaging* 2016;43:512-32.
 73. Manes A, Campana C. Pulmonary hypertension: Classification and diagnostic algorithm. *Ital Heart J* 2005;6:834-9.
 74. Tonelli AR, Yadav R, Gupta A, Arrossi AV, Heresi GA, Dweik RA. Spleen size in idiopathic and heritable pulmonary arterial hypertension. *Respiration* 2013;85:391-9.
 75. Di Carli MF, Kwong RY, Solomon SD. Noninvasive cardiac imaging: Echocardiography, nuclear cardiology, and magnetic resonance/computed tomography imaging. In: Kasper D, Fauci A, Hauser S, Longo D, Jameson J, Loscalzo J, editors. *Harrison's Principles of Internal Medicine*. 19th ed. New York: McGraw-Hill; 2015. Available from: <http://www.accessmedicine.mhmedical.com/content.aspx?bookid=1130&Sectionid=79741825>. [Last accessed on 2016 May 27].
 76. Kawakami T, Kataoka M, Nakahara T, Yamada Y, Takei M, Jinzaki M, et al. Usefulness of 3D SPECT/CT fusion image in CTEPH. *Int J Cardiol* 2015;194:39-40.
 77. Mazurek A, Dziuk M, Witkowska-Patena E, Piszczek S, Gizewska A. The utility of hybrid SPECT/CT lung perfusion scintigraphy in pulmonary embolism diagnosis. *Respiration* 2015;90:393-401.
 78. Lysenkov Mlu, Ansheles AA, Ivanov KP, Martyniuk TV, Sergienko VB. Diagnostic capabilities of single-photon emission computed tomography/computed tomography in the evaluation of perfusion disorders in pulmonary hypertension. *Vestn Rentgenol Radiol*. 2013;(6):26-31.
 79. Lau EM, Bailey DL, Bailey EA, Torzillo PJ, Roach PJ, Schembri GP, et al. Pulmonary hypertension leads to a loss of gravity dependent redistribution of regional lung perfusion: A SPECT/CT study. *Heart* 2014;100:47-53.
 80. Soler X, Hoh CK, Test VJ, Kerr KM, Marsh JJ, Morris TA. Single photon emission computed tomography in chronic thromboembolic pulmonary hypertension. *Respirology* 2011;16:131-7.

81. Ameli-Renani S, Rahman F, Nair A, Ramsay L, Bacon JL, Weller A, *et al.* Dual-energy CT for imaging of pulmonary hypertension: Challenges and opportunities. *Radiographics* 2014;34:1769-90.
82. Hachulla AL, Lador F, Soccal PM, Montet X, Beghetti M. Dual-energy computed tomographic imaging of pulmonary hypertension. *Swiss Med Wkly* 2016;146:w14328.
83. Apfalter P, Bachmann V, Meyer M, Henzler T, Barraza JM, Gruettner J, *et al.* Prognostic value of perfusion defect volume at dual energy CTA in patients with pulmonary embolism: Correlation with CTA obstruction scores, CT parameters of right ventricular dysfunction and adverse clinical outcome. *Eur J Radiol* 2012;81:3592-7.
84. Okada M, Kunihiro Y, Nakashima Y, Nomura T, Kudomi S, Yonezawa T, *et al.* Added value of lung perfused blood volume images using dual-energy CT for assessment of acute pulmonary embolism. *Eur J Radiol* 2015;84:172-7.
85. Bauer RW, Frellesen C, Renker M, Schell B, Lehnert T, Ackermann H, *et al.* Dual energy CT pulmonary blood volume assessment in acute pulmonary embolism – Correlation with D-dimer level, right heart strain and clinical outcome. *Eur Radiol* 2011;21:1914-21.
86. Meinel FG, Graef A, Thierfelder KM, Armbruster M, Schild C, Neurohr C, *et al.* Automated quantification of pulmonary perfused blood volume by dual-energy CTPA in chronic thromboembolic pulmonary hypertension. *Rofo* 2014;186:151-6.
87. Hong YJ, Kim JY, Choe KO, Hur J, Lee HJ, Choi BW, *et al.* Different perfusion pattern between acute and chronic pulmonary thromboembolism: Evaluation with two-phase dual-energy perfusion CT. *AJR Am J Roentgenol* 2013;200:812-7.
88. Wirth G, Brüggemann K, Bostel T, Mayer E, Düber C, Kreitner KF. Chronic thromboembolic pulmonary hypertension (CTEPH) – Potential role of multidetector-row CT (MD-CT) and MR imaging in the diagnosis and differential diagnosis of the disease. *Rofo* 2014;186:751-61.
89. García-Álvarez A, García-Lunar I, Pereda D, Fernández-Jimenez R, Sánchez-González J, Mirelis JG, *et al.* Association of myocardial T1-mapping CMR with hemodynamics and RV performance in pulmonary hypertension. *JACC Cardiovasc Imaging* 2015;8:76-82.
90. Nordmeyer S, Riesenkampff E, Messroghli D, Kropf S, Nordmeyer J, Berger F, *et al.* Four-dimensional velocity-encoded magnetic resonance imaging improves blood flow quantification in patients with complex accelerated flow. *J Magn Reson Imaging* 2013;37:208-16.
91. Reiter U, Reiter G, Kovacs G, Stalder AF, Gulsun MA, Greiser A, *et al.* Evaluation of elevated mean pulmonary arterial pressure based on magnetic resonance 4D velocity mapping: Comparison of visualization techniques. *PLoS One* 2013;8:e82212.
92. François CJ, Srinivasan S, Schiebler ML, Reeder SB, Niespodzany E, Landgraf BR, *et al.* 4D cardiovascular magnetic resonance velocity mapping of alterations of right heart flow patterns and main pulmonary artery hemodynamics in tetralogy of Fallot. *J Cardiovasc Magn Reson* 2012;14:16.
93. Geiger J, Markl M, Jung B, Grohmann J, Stiller B, Langer M, *et al.* 4D-MR flow analysis in patients after repair for tetralogy of Fallot. *Eur Radiol* 2011;21:1651-7.
94. Roldán-Alzate A, Frydrychowicz A, Johnson KM, Kelliham H, Chesler NC, Wieben O, *et al.* Non-invasive assessment of cardiac function and pulmonary vascular resistance in a canine model of acute thromboembolic pulmonary hypertension using 4D flow cardiovascular magnetic resonance. *J Cardiovasc Magn Reson* 2014;16:23.
95. Nordmeyer S, Riesenkampff E, Crelier G, Khasheei A, Schnackenburg B, Berger F, *et al.* Flow-sensitive four-dimensional cine magnetic resonance imaging for offline blood flow quantification in multiple vessels: A validation study. *J Magn Reson Imaging* 2010;32:677-83.
96. Markl M, Wallis W, Harloff A. Reproducibility of flow and wall shear stress analysis using flow-sensitive four-dimensional MRI. *J Magn Reson Imaging* 2011;33:988-94.
97. Mauritz GJ, Vonk-Noordegraaf A, Kind T, Surie S, Kloek JJ, Bresser P, *et al.* Pulmonary endarterectomy normalizes interventricular dyssynchrony and right ventricular systolic wall stress. *J Cardiovasc Magn Reson* 2012;14:5.